THE ASTROPHYSICAL JOURNAL, 576:L169–L172, 2002 September 10
© 2002. The American Astronomical Society. All rights reserved. Printed in U.S.A.

LABORATORY MEASUREMENTS OF THE RELATIVE INTENSITY OF THE $3s \rightarrow 2p$ AND $3d \rightarrow 2p$ TRANSITIONS IN Fe XVII

P. BEIERSDORFER,[1] E. BEHAR,[2] K. R. BOYCE,[3] G. V. BROWN,[3] H. CHEN,[1] K. C. GENDREAU,[3] M.-F. GU,[4] J. GYGAX,[3] S. M. KAHN,[2] R. L. KELLEY,[3] F. S. PORTER,[3] C. K. STAHLE,[3] AND A. E. SZYMKOWIAK[3]
Received 2002 March 16; accepted 2002 July 30; published 2002 August 20

ABSTRACT

The intensity ratios of the $3s \rightarrow 2p$ and $3d \rightarrow 2p$ lines in Fe XVII were measured on the Livermore electron beam ion trap employing a complementary set of spectrometers, including a high-resolution crystal spectrometer and the Goddard 32 pixel calorimeter. The resulting laboratory data are in agreement with satellite measurements of the Sun and astrophysical sources in collisional equilibrium such as Capella, Procyon, and NGC 4636. The results disagree with earlier laboratory measurements and assertions that processes not accounted for in laboratory measurements must play a role in the formation of the Fe XVII spectra in solar and astrophysical plasmas.

Subject headings: atomic data — stars: coronae — stars: individual (Capella, Procyon) — Sun: X-rays, gamma rays — X-rays: general

1. INTRODUCTION

The emission from Fe XVII dominates the iron L-shell spectrum in the temperature range from 1 to 7 MK and thus is a very important component for spectral diagnostics. The spectrum contains three $3d \rightarrow 2p$ and three $3s \rightarrow 2p$ transitions. The first three correspond to the electric dipole-allowed transitions from upper levels $(2p^5_{1/2}3d_{3/2})_{J=1}$, $(2p^5_{3/2}3d_{5/2})_{J=1}$, and $(2p^5_{3/2}3d_{3/2})_{J=1}$ to the $(2p^6)_{J=0}$ ground state and are commonly labeled 3C, 3D, and 3E, respectively. Two more, labeled 3F and 3G, correspond to the electric dipole-allowed transitions from upper levels $(2p^5_{1/2}3s_{1/2})_{J=1}$ and $(2p^5_{3/2}3s_{1/2})_{J=1}$, respectively, to the Fe XVII ground state. The last, labeled M2, arises from the magnetic quadrupole decay of the $(2p^5_{1/2}3s_{1/2})_{J=2}$ upper level to ground. These lines have been observed in the Sun, (e.g., Parkinson 1975; McKenzie et al. 1980; Phillips et al. 1982) as well as in numerous cosmic sources studied with the *Chandra* and *XMM-Newton* observatories (e.g., Canizares et al. 2000; Brinkman et al. 2000; Behar, Cottam, & Kahn 2001; Raassen et al. 2002; Xu et al. 2002).

The diagnostic utility of the Fe XVII spectrum has been limited, as atomic models have not been able to reproduce the observations. Advances in laboratory astrophysics, however, have started to overcome these limitations. One issue was the intensity ratio of the 3C and 3D lines observed in solar and astrophysical sources that was well below the calculated values, leading to speculation that opacity effects may affect this line ratio (Saba et al. 1999). Using high-resolution crystal spectrometers, our laboratory astrophysics program showed that the "low" intensity ratio is in large part an artifact of the atomic data, which overestimated this ratio (Brown et al. 1998, 2001a; Brown, Beiersdorfer, & Widmann 2001b; Beiersdorfer et al. 2001) so that opacity effects in many cases do not need to be invoked to model this ratio. Moreover, we also showed that the ratio is reduced by line blending with at least one or more Fe XVI lines, depending on the spectral resolution (Brown et al. 2001a; Behar et al. 2001).

A major remaining issue is the ratio $I_{3s\rightarrow 2p}/I_{3d\rightarrow 2p}$ of the $3s \rightarrow 2p$ lines to the $3d \rightarrow 2p$ lines. In most astrophysical sources this ratio is found to be consistently larger than calculations. For example, a study of data collected as part of the *Solar Maximum Mission* required an increase of the predicted flux of lines 3F, 3G, and M2 relative to that of 3C by about 50% (Phillips et al. 1999). Understanding whether this discrepancy is caused by source physics or merely errors in the atomic data is critical and has wide-reaching implications for their diagnostic use.

In the following, we present measurements of $I_{3s\rightarrow 2p}/I_{3d\rightarrow 2p}$. Our results are in good agreement with the ratios from solar and astrophysical collisional plasmas where electron-impact ionization is the dominant excitation mechanism. We therefore find that no special source-related processes not found in the laboratory are necessary to explain the observational data.

2. MEASUREMENT

The present measurements were performed on the Lawrence Livermore National Laboratory (LLNL) electron beam ion trap EBIT-II. This is the second such device, producing laboratory data used in atomic codes since 1990. The device includes a unique suite of spectrometers optimized for multiwavelength laboratory astrophysics measurements. We employed three sets of instruments to observe the Fe XVII spectrum: a broadband crystal spectrometer (Brown, Beiersdorfer, & Widmann 1999), a flat-field grazing-incidence spectrometer with charge-coupled device readout (Utter et al. 1999), and the 32 pixel Goddard microcalorimeter (Porter et al. 2000). While this suite of instrumentation may seem more than sufficient, we deemed this imperative given that we wanted to firmly determine the correct Fe XVII line ratios.

All three of our instruments were carefully calibrated. The calibration procedure of the crystal spectrometer was described by Brown et al. (1998) and extended to include the long-wavelength region well beyond 17 Å. The present measurements recorded the $3d \rightarrow 2p$ and $3s \rightarrow 2p$ lines on a single detector from a single rubidium acid-phthalate crystal. The microcalorimeter represented the engineering model X-ray spectrometer (XRS) of the *Astro-E* mission and was thoroughly calibrated in that capacity (Audley et al. 1999; Gendreau et al. 1999). Furthermore, in situ calibrations were performed while operating on EBIT-II with an X-ray tube to monitor the possibility of ice buildup on the infrared blocking filters while cold. The flat-field spectrometer was calibrated for wavelengths above 10 Å at the Advanced Light Source synchrotron. Moreover, the calibration was checked

[1] University of California Lawrence Livermore National Laboratory, 7000 East Avenue, Livermore, CA 94551.
[2] Columbia Astrophysics Laboratory, Columbia University, 550 West 120th Street, New York, NY 10027.
[3] NASA Goddard Space Flight Center, Greenbelt, MD 20770.
[4] Center for Space Research, Massachusetts Institute of Technology, 70 Vassar Street, Cambridge, MA 02139.

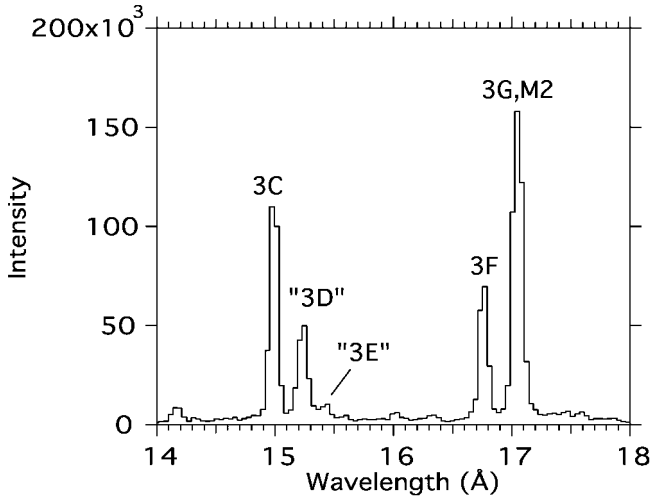

FIG. 1.—Fe XVII emission recorded on EBIT-II with a grazing-incidence grating spectrometer at an electron beam energy of 1.13 keV. A nonequilibrium abundance of Fe XVI was generated in the trap to demonstrate the enhancement of lines 3D and 3E through blending with Fe XVI and Fe XV.

in situ by recording the O VIII Lyman series and making use of the predicted intensity pattern (Smith et al. 2001).

To probe possible variations of the Fe XVII lines, our measurements were carried out at different beam energies, with equilibrium and nonequilibrium ionization balances, and various levels of background oxygen impurities. The XRS calorimeter provided superior throughput and thus collected spectra much faster than the grating or crystal spectrometer. However, the higher resolution of the crystal spectrometer was necessary to account for line blends in the XRS and grating spectra. Typical spectra obtained with our three instruments are shown in Figures 1–3. The spectra shown were corrected for instrumental response but not for the polarization effects discussed below.

The ratios must be adjusted for the fact that the lines excited by an electron beam are polarized and emitted spatially anisotropic. In line with our earlier measurements and with calculations (Utter et al. 1999; Zhang, Sampson, & Clark 1990), we set the polarization $P = 0.40$ for 3C and 3D, $P = -0.40$ for 3E, $P = 0.20$ for 3F, and $P = 0$ for 3G and M2. This changes $I_{3s\rightarrow 2p}/I_{3d\rightarrow 2p}$ by a factor of 1.13. In addition, the crystal measurements must be adjusted for the polarization-dependent reflectivity response (Henke, Gullikson, & Davis 1993).

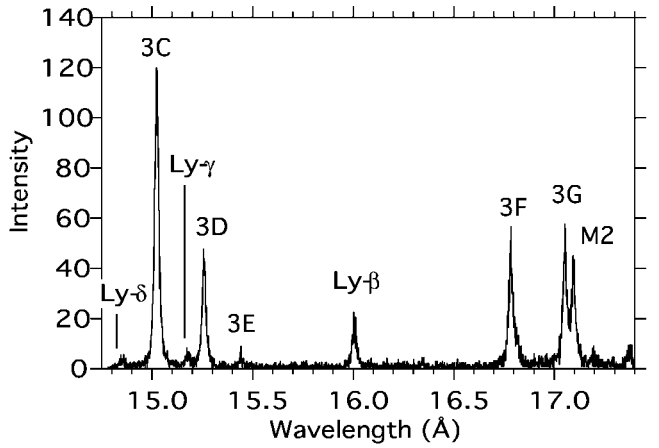

FIG. 2.—Fe XVII emission recorded on EBIT-II with a flat-crystal spectrometer at an electron beam energy of 1.13 keV. Also seen are the Lyβ, Lyγ, and Lyδ lines from O VIII.

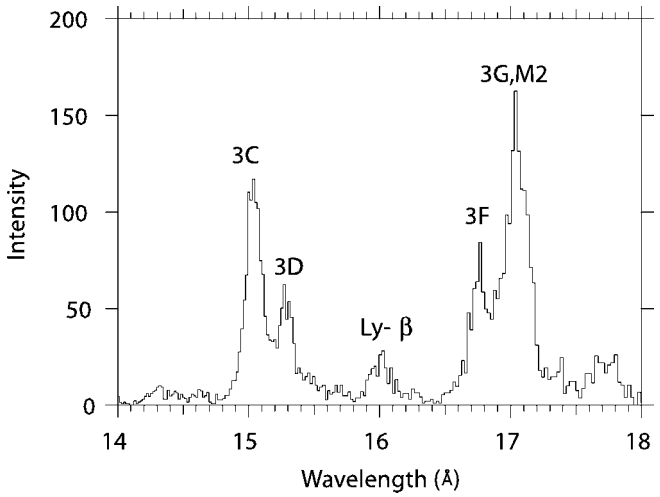

FIG. 3.—Fe XVII emission recorded on EBIT-II with the Goddard X-ray microcalorimeter at an electron beam energy of 0.93 keV. Lyβ denotes the $3p \rightarrow 1s$ transition in O VIII.

A summary of the $I_{3s\rightarrow 2p}/I_{3d\rightarrow 2p}$ ratios inferred from our measurements is shown in Figure 4. In many situations, the intensity of the $3s \rightarrow 2p$ lines relative to that of 3C, $I_{3s\rightarrow 2p}/I_{3C}$, is a better diagnostic ratio than $I_{3s\rightarrow 2p}/I_{3d\rightarrow 2p}$. The reason is that lines 3D and 3E are weak and readily blended with lines from lower charge states of iron, depending on the resolving power of the measurement. The $I_{3s\rightarrow 2p}/I_{3C}$ ratio is summarized in Table 1 and plotted in Figure 5.

Owing to the intrinsic strength of the lines studied, statistics contribute little (<1%) to the uncertainties in the measured ratios. Instead, the uncertainties are dominated by systematics associated with each instrument. An uncertainty common to all measurements is the level of polarization. Assuming $P = 0$ instead of $P = 0.20$ for 3F because of resonance and cascade contributions, for example, increases the adjustment factor by 2% to 1.15. The thermal properties of the electron beam have the effect of reducing the amount of polarization of each line. The thermal component of the beam energy may range from 110 to 200 eV under standard operating conditions (Beiersdorfer et al. 1992; Beiersdorfer & Slater 2001). The latter will reduce the polarization of 3C from $P = 0.40$ to about $P = 0.30$ and the overall

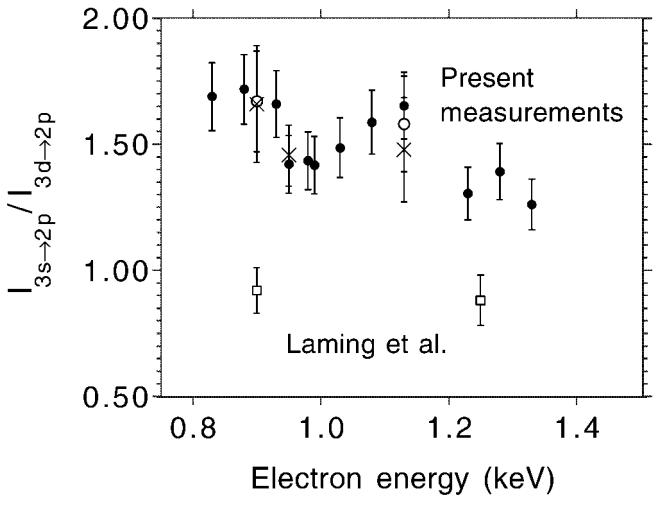

FIG. 4.—Measured $3s \rightarrow 2p$ to $3d \rightarrow 2p$ line intensities vs. electron energy. *Filled circles*: Goddard X-ray calorimeter. *Crosses*: crystal spectrometer. *Open circles*: Grating spectrometer. *Open squares*: SAO calorimeter (Laming et al. 2000).

TABLE 1

$I_{3s\rightarrow 2p}/I_{3C}$ MEASURED AS A FUNCTION OF ELECTRON ENERGY

Energy (keV)	Unadjusted Ratio	Polarization-adjusted Ratio
	XRS Calorimeter	
0.83	2.08	2.33
0.88	2.12	2.37
0.93	2.04	2.29
0.95	1.96	1.96[a]
0.98	1.77	1.98
0.99	1.73	1.96
1.03	1.83	2.05
1.08	1.95	2.19
1.13	2.04	2.28
1.23	1.61	1.80
1.28	1.71	1.92
1.33	1.55	1.74
	Grating Spectrometer	
0.90	2.04	2.30
1.13	1.93	2.18
	Crystal Spectrometer	
0.90	1.48	2.29
0.95	2.01	2.01[a]
1.13	1.32	2.04

[a] Nearly unpolarized beam; no polarization adjustment.

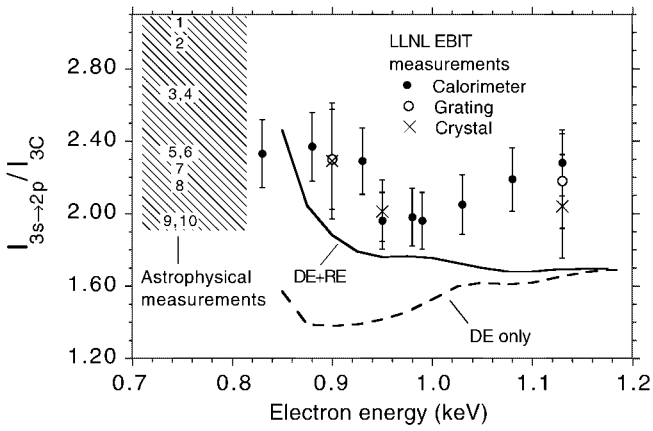

FIG. 5.—Intensities of the $3s \rightarrow 2p$ transitions relative to line 3C vs. electron energy. Model calculations using the FAC code (Gu 2002) with and without resonant excitation are shown as solid and dashed lines, respectively; both are convolved with a 30 eV spread in the electron beam energy. Also shown is the range of observational values, which is indicated by the hatched region on the left. Specific observations are labeled by number. In the astrophysical cases, the lines may be emitted over a range of temperatures, so that the location in electron energy is not especially clear. The energy scale on the *x*-axis should be, therefore, disregarded for these. In collisional ionization equilibrium, however, the Fe XVII emission is dominated by collisions with electrons near the excitation threshold. Legend: (1) Raassen et al. (2002; Procyon); (2) McKenzie et al. (1980; Sun); (3, 4) Hutcheon, Pye, & Evans (1976; Sun); (5) Behar et al. (2001; Capella); (6) Canizares et al. (2000; Capella); (7) Xu et al. (2002; NGC 4636); (8) Raassen et al. (2002; Procyon); (9) Brinkman et al. (2000; Capella); (10) Hutcheon et al. (1976; Sun).

polarization adjustment factor by about 5%. To these uncertainties we add in quadrature the systematic uncertainties associated with each instrument. In the case of the XRS measurements, we estimate a 6% uncertainty in the line fitting due to unresolved oxygen lines as well as a 2% uncertainty in the foil absorption (detection efficiency) calibration, which gives an 8% overall systematic uncertainty. For the grating measurements, we estimate a 9% uncertainty in the reflectivity response and a 6% uncertainty in the line fitting for a 12% overall uncertainty. The estimated uncertainties of the crystal measurements include a 1% differential crystal reflectivity response uncertainty, a 5% foil transmission uncertainty, and a less than 1% uncertainty for line fitting. The largest uncertainty, 12%, results from polarization-dependent reflectivity response due to the uncertainty in the assumed polarization. The total systematic uncertainty is 14%.

After polarization adjustment, the results of all three instruments agree with each other better than their respective uncertainty limits. This agreement not only validates the assumed polarization values but also indicates that the assumed uncertainty in the line polarizations is likely to be overestimated.

Our attempt to cover a wide parameter space included one measurement where we detuned the electron beam to increase the perpendicular energy component of the beam to a point where we believe that there were little or no polarization effects. In this case, we made no adjustments for polarization (see Table 1). In the absence of polarization corrections, these two points represent a *lower limit* of the $I_{3s\rightarrow 2p}/I_{3d\rightarrow 2p}$ ratio. This lower limit agrees well with the values obtained assuming full polarization, again validating our polarization assumptions.

When generating a nonequilibrium fraction of Fe XVI to observe the effect of lower charge states on the Fe XVII lines, we find that a high Fe XVI abundance strongly enhances not only the apparent 3D line but also the apparent 3E line in the grating and calorimeter observations (see Fig. 1). Both of these features, therefore, serve as indicators of the presence of low-charge states of iron in moderate-resolution measurements. In the absence of Fe XVI, we measured a ratio ranging from $I_{3E}/I_{3C} \approx 0.04 \pm 0.01$ to $I_{3E}/I_{3C} \approx 0.06 \pm 0.02$ with the crystal spectrometer for different beam energies. (This ratio was multiplied by a factor of 2.6 to account for polarization effects.) Provided the beam energy is below the threshold for inner-shell ionization of neon-like iron, i.e., the removal of a $2p$ or $2s$ electron above 1210 eV, the other four Fe XVII lines remain unchanged.

3. DISCUSSION

A recent laboratory measurement of the ratio of the $3s \rightarrow 2p$ to $3d \rightarrow 2p$ lines reported by Laming et al. (2000) used the National Institute of Standards and Technology (NIST) electron beam ion trap and the Smithsonian Astrophysical Observatory (SAO) single-pixel X-ray calorimeter to measure the Fe XVII spectrum at several fixed electron excitation energies. From these measurements, they determined that the ratio $I_{3s\rightarrow 2p}/I_{3d\rightarrow 2p}$ was in good agreement with calculations and that "the basic electron impact excitation theory for these lines in Fe XVII appears to be correct." Their theory and their laboratory data, however, differed by nearly a factor of 2 from the $I_{3s\rightarrow 2p}/I_{3d\rightarrow 2p}$ ratio measured from the Sun and Capella. Their result would have far-reaching consequences for solar and astrophysics. In a subsequent paper, the measured ratios by the NRL-NIST-SAO collaboration were even smaller (Kink et al. 2001), further increasing the discrepancy with the astrophysical and solar ratios.

Our measurements strongly disagree with the laboratory data presented by Laming et al. (2000), as shown by the comparison with their results in Figure 4. Near excitation threshold, which typically dominates the line emission in a collisional plasma in equilibrium, the difference between their values and ours is nearly a factor of 2.

In Figure 5, we compare our $I_{3s\rightarrow 2p}/I_{3C}$ ratios with the ratios obtained from various solar and astrophysical observations. Unlike the Laming et al. (2000) values, our values are in very good agreement with those from collisional astrophysical and solar plasmas. This agreement demonstrates that the assertion by Laming et al. that "one must look to other processes to model the solar and astrophysical observations satisfactorily"

is moot. There is no need to invoke as of yet unidentified processes that are absent in the laboratory to explain the astrophysical observations.

To understand the source of the disagreement with the NRL-NIST-SAO data, we point out differences between our measurement and theirs. Laming et al. (2000) assert that the NIST electron beam ion trap operates "under similar conditions" as the LLNL electron beam ion trap. However, the NIST electron beam ion trap does not operate below 700 eV (Takács et al. 1996; Gillaspy 1996), while our device does not have such performance limitations, perhaps because our machine typically operates at significantly lower beam temperatures than the NIST device (Beiersdorfer et al. 1992, 1999; Beiersdorfer & Slater 2001). Moreover, the uncertainty in the actual electron beam energy is negligible, as the space charge is measured, not calculated (e.g., Gu et al. 2001). Fe XVII burns out in our device above about 1500 eV in a monoenergetic electron beam plasma. This is expected from the ionization potentials of Fe XVII, Fe XVIII, and Fe XIX, which are 1262, 1358, and 1456 eV, respectively, and confirmed by ionization balance calculations (Beiersdorfer et al. 2000). The fact that the NRL-SAO-NIST measurements observed Fe XVII as high as 4 keV (Laming et al. 2000; Kink et al. 2001) and even 10 keV (Silver et al. 2000) indicates that their results were obtained under different plasma conditions from our measurements and that the NIST electron beam ion trap may not operate in collisional equilibrium. Moreover, the SAO calorimeter did not provide time-resolved data (J. M. Laming & E. Takács 2002, private communication); as a consequence, their calorimeter integrated the ionization, recombination, and steady state phases alike. The nonequilibrium conditions in the Laming et al. measurements were already pointed out by Brown et al. (2001a), who showed that a substantial fraction of Fe XVI contaminated the Laming et al. value of the 3C/3D intensity ratio, reducing their ratio substantially below the uncontaminated, collisional value measured at LLNL. Similarly, the value of 0.10 obtained by Laming et al. for the ratio of I_{3E}/I_{3C} is twice the value we measure in ionization equilibrium. Laming et al. did not have access to high-resolution spectrometers needed to discern line blends. In addition, their calorimeter response was not calibrated or monitored in situ (J. M. Laming & E. Takacs 2002, private communication).

Finally, we compare in Figure 5 our experimental data with a new Fe XVII model calculation using the FAC code (Gu 2002). Two calculations are shown. In the first, electron-impact excitation and radiative cascades are the only line formation processes. This calculation includes cascades from levels with principal quantum number as high as $n = 7$. Cascades from the higher n levels have the effect of increasing $I_{3s\rightarrow 2p}/I_{3C}$ as a function of electron energy. The second calculation additionally includes resonance excitation, which is computed in the isolated resonance approximation. Doubly excited configurations of the type $(2s,\ 2p)^7 3lnl'$ and $(2s,\ 2p)^7 4lnl'$ with $n \leq 20$ are included. The present resonant excitation rate coefficients appear to be ≈50% higher than Goldstein et al. (1989) and Chen & Reed (1989) for the $3s$ and $3p$ levels. The detail of the calculation for Fe XVII and other Fe L-shell ions will be presented in a later publication (Gu 2002). Inclusion of resonance excitation brings better agreement with our measurements. This is expected, as resonance excitation is an integral part of the line formation process. But the agreement is not yet perfect.

Work by the University of California LLNL was performed under contract W-7405-Eng-48 and supported by the NASA Space Astrophysics Research and Analysis Program under work order S-03958G and grant NAG5-5123. We thank Eric Gullikson for his support at the Advanced Light Source. M.-F. G. is supported by NASA through *Chandra* Postdoctoral Fellowship Award number PF01-10014 issued by the *Chandra X-Ray Observatory* Center, which is operated by the SAO for and on behalf of NASA under contract NAS8-39073. This work was performed while G. V. B. held an NRC Associateship Award at GSFC.

REFERENCES

Audley, M. D., et al. 1999, Proc. SPIE, 3765, 751
Behar, E., Cottam, J., & Kahn, S. M. 2001, ApJ, 548, 966
Beiersdorfer, P., Lepson, J. K., Brown, G. V., Utter, S. B., Kahn, S. M., Liedahl, D. A., & Mauche, C. W. 1999, ApJ, 519, L185
Beiersdorfer, P., Phillips, T. W., Wong, K. L., Marrs, R. E., & Vogel, D. A. 1992, Phys. Rev. A, 46, 3812
Beiersdorfer, P., & Slater, M. 2001, Phys. Rev. E, 64, 066408
Beiersdorfer, P., von Goeler, S., Bitter, M., & Thorn, D. B. 2001, Phys. Rev. A, 64, 032705
Beiersdorfer, P., et al. 2000, Rev. Mexicana Astron. Astrofis. Ser. Conf., 9, 123
Brinkman, A. C., et al. 2000, ApJ, 530, L111
Brown, G. V., Beiersdorfer, P., Chen, H., Chen, M. H., & Reed, K. J. 2001a, ApJ, 557, L75
Brown, G. V., Beiersdorfer, P., Kahn, S., Liedahl, D., & Widmann, K. 1998, ApJ, 502, 1015
Brown, G. V., Beiersdorfer, P., & Widmann, K. 1999, Rev. Sci. Instrum., 70, 280
———. 2001b, Phys. Rev. A, 63, 032719
Canizares, C. R., et al. 2000, ApJ, 539, L41
Chen, M. H., & Reed, K. J. 1989, Phys. Rev. A, 40, 2292
Gendreau, K. C., et al. 1999, Proc. SPIE, 3765, 137
Gillaspy, J. D. 1996, Phys. Scr., T65, 168
Goldstein, W. H., Osterheld, A., Oreg, J., & Bar-Shalom, A. 1989, ApJ, 344, L37
Gu, M.-F. 2002, ApJ, submitted
Gu, M.-F., Kahn, S. M., Savin, D. W., Behar, E., Beiersdorfer, P., Brown, G. V., Liedahl, D. A., & Reed, K. J. 2001, ApJ, 563, 462
Henke, B. L., Gullikson, E. M., & Davis, J. C. 1993, At. Data Nucl. Data Tables, 54, 181
Hutcheon, R. J., Pye, J. P., & Evans, K. D. 1976, MNRAS, 175, 489
Kink, I., et al. 2001, Phys. Scr., T92, 454
Laming, J. M., et al. 2000, ApJ, 545, L161
McKenzie, D. L., Landecker, P. B., Broussard, R. M., Rugge, H. R., Young, R. M., Feldman, U., & Doschek, G. A. 1980, ApJ, 241, 409
Parkinson, J. H. 1975, Sol. Phys., 42, 183
Phillips, K. J. H., Mewe, R., Harra-Murnion, L. K., Kaastra, J. S., Beiersdorfer, P., Brown, G. V., & Liedahl, D. A. 1999, A&AS, 138, 381
Phillips, K. J. H., et al. 1982, ApJ, 256, 774
Porter, F. S., et al. 2000, Proc. SPIE, 4140, 407
Raassen, A. J. J., et al. 2002, A&A, in press
Saba, J. L. R., Schmelz, J. Y., Bhatia, A. K., & Strong, K. T. 1999, ApJ, 510, 1064
Silver, E., et al. 2000, BAAS, 32, 12.65
Smith, R. K., Brickhouse, N. S., Liedahl, D. A., & Raymond, J. C. 2001, ApJ, 556, L91
Takács, E., et al. 1996, Phys. Rev. A, 54, 1342
Utter, S. B., Brown, G. V., Beiersdorfer, P., Clothiaux, E. J., & Podder, N. K. 1999, Rev. Sci. Instrum., 70, 284
Xu, H., Kahn, S. M., Peterson, J. R., Behar, E., Paerels, F. B. S., Mushotzky, R. F., Jernigan, J. G., & Makishima, K. 2002, ApJ, in press
Zhang, H. L., Sampson, D. H., & Clark, R. E. H. 1990, Phys. Rev. A, 41, 198